Earth and Planetary Science Letters 546 (2020) 116415

Contents lists available at ScienceDirect

Earth and Planetary Science Letters

www.elsevier.com/locate/epsl

# Multiple measures of monsoon-controlled water storage in Asia

Amanda H. Schmidt [a,*], Stefan Lüdtke [b], Christoff Andermann [c]

[a] Geology Department, Oberlin College, 403 Carnegie Building, 52 W. Lorain St., Oberlin, OH 44074, United States
[b] Helmholtz Centre Potsdam, GFZ German Research Centre for Geosciences, Section 4.4 Hydrology, Telegrafenberg, 14473 Potsdam, Germany
[c] Helmholtz Centre Potsdam, GFZ German Research Centre for Geosciences, Section 4.6 Geomorphology, Telegrafenberg, 14473 Potsdam, Germany

ARTICLE INFO

*Article history:*
Received 3 January 2020
Received in revised form 8 June 2020
Accepted 9 June 2020
Available online xxxx
Editor: L. Derry

*Keywords:*
recession curve
dynamic storage
transient storage
groundwater
GRACE

ABSTRACT

Temporal water storage is a fundamental component of the terrestrial water cycle. Methods of estimating water storage variations are often limited to specific, well-monitored locations, and/or system scales. Thus, measures of storage from small systems can be difficult to compare to large systems. Here we compare three independent methods of estimating water storage variations for systems spanning over three orders of magnitude in basin area: 1) remote satellite observations (GRACE), 2) hydrograph recession curve analysis, and 3) quantifying precipitation-discharge hysteresis loops. We measured storage using all three methods for 242 watersheds in Asia ($10^3$ to $10^6$ km$^2$) and find that GRACE-derived storage correlates well with quantification of hysteresis terms but recession curve derived dynamic storage does not correlate with hysteresis terms or GRACE-derived storage. Thus, we argue that precipitation-discharge hysteresis may be able to be scaled to GRACE-derived storage as an independent estimate of storage for basins as small as $10^3$ km$^2$. Hysteresis-derived storage correlates well with mean monsoon rainfall in the upstream watershed while recession-derived dynamic storage does not. This suggests that hysteresis- and GRACE-derived storage may be input limited. In contrast, recession-derived dynamic storage does not correlate with topographic, climatic, or land cover metrics, suggesting that it may be limited by the rate at which water infiltrates into deep groundwater and then enters the river system. In addition, we find that recession-derived dynamic storage is a factor of seven lower than hysteresis-derived storage. We infer that hysteresis-derived storage includes recession curve-derived storage in addition to other storage units, such as snowpack, lakes, and soil moisture. Recession-derived dynamic storage in turn represents the annual variability in deep groundwater storage, a "leaky bucket" that is recharged from the top and "leaks" into rivers from deeper storage. These data may be able to be used to better quantify storage terms in hydrologic modeling.



## 1. Introduction

Understanding the highly complex routes by which water is transferred from precipitation to river discharge is essential to understanding the continental water cycle (Jasechko et al., 2016). The majority of precipitation falling on Earth is transferred via surface runoff or groundwater through a series of short- to long-term storage locations, then to the rivers, and eventually ends in the oceans or, through evapotranspiration, back in the atmosphere (Oki and Kanae, 2006). Although the water cycle is conceptually well described (e.g., Gleeson et al., 2016), the dynamics, amplitudes of fluctuation, and locations of storage are not well constrained (Taylor et al., 2013) and are the subject of ongoing debate (McDonnell, 2017).

Water is stored in a variety of landscape locations, including lakes, snow and ice, soil moisture, shallow and deep groundwater, floodplains, wetlands, and rivers. Approximately 30% of global freshwater is stored as groundwater ($2.2–2.3 \times 10^7$ km$^3$) (Gleeson et al., 2016; Oki and Kanae, 2006), which is subdivided into a deep groundwater saturated zone and the relatively shallow unsaturated (vadose) zone. Some of the water from the shallow vadose zone infiltrates and recharges the deep groundwater. This is the source of river water when there has not been recent precipitation. Conceptually this is considered a "leaky bucket" groundwater model (Manabe, 1969). The relative distribution of continental freshwater between storage locations is uneven across Earth and fluxes between storage sites, including the ocean and atmosphere, vary considerably in both space and time; this variability is poorly con-

* Corresponding author.
*E-mail addresses:* aschmidt@oberlin.edu (A.H. Schmidt), stefan.luedtke@gfz-potsdam.de (S. Lüdtke), christoff.andermann@gfz-potsdam.de (C. Andermann).

https://doi.org/10.1016/j.epsl.2020.116415
0012-821X/

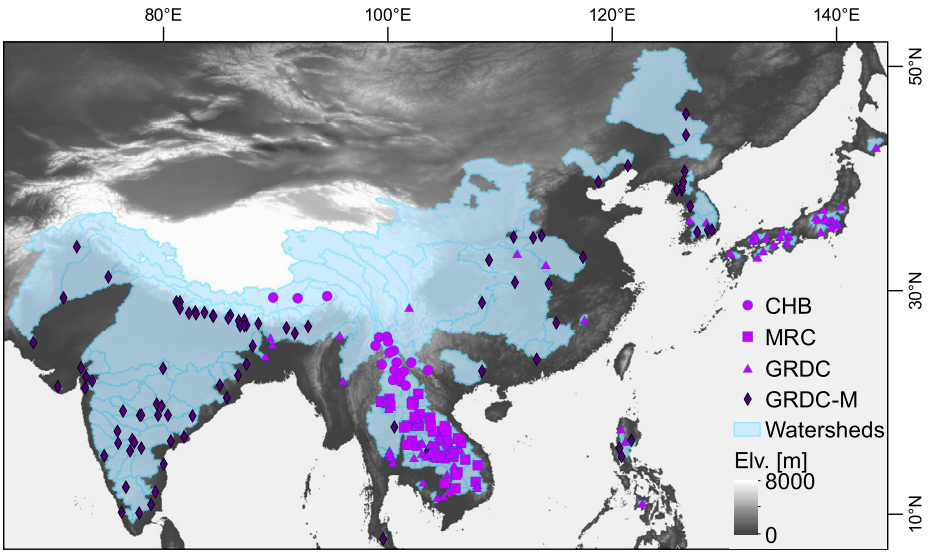


**Fig. 1.** Locations of hydrology stations used in analysis on a background of elevation data (USGS, 2008). Stations are identified by the dataset their discharge data is from – the Chinese Hydrology Bureau (circles; CHB), Mekong River Commission (squares; MRC), or Global Rivers Data Centre daily (triangles; GRDC) and monthly (diamonds; GRDC-M) datasets (GRDC, 2015; Henck et al., 2010; MRC, 2015). Stations with daily data are in light purple and stations with monthly data in dark purple. (For interpretation of the colors in the figure(s), the reader is referred to the web version of this article.)

strained (McDonnell, 2017; Oki and Kanae, 2006). Furthermore, within individual storage units, such as groundwater, the distribution between subunits is relatively poorly quantified (Gleeson et al., 2016). Recent findings suggest that a large portion of infiltrated water never reaches the saturated groundwater zone but is retained close to the surface, in biomass or in the vadose zone, and some fraction evaporates back into the atmosphere (Dralle et al., 2018). In addition, water in rock fractures and pockets in the vadose zone may be an important source of water for both plants and streamflow through the dry season (Rempe and Dietrich, 2018).

Spatially integrated measurements of storage typically rely on satellite data (e.g., Scanlon et al., 2018; Strassberg et al., 2007), interpolated point observations of boreholes (e.g., Rodell et al., 2007), GPS inversions (e.g., Fu et al., 2015), recession curve analysis (e.g., Brutsaert and Nieber, 1977; Kirchner, 2009), and/or hydrologic modeling (e.g., Scanlon et al., 2018). Different techniques may measure different compartments of water storage. In addition, prior work suggests that the lag of river discharge with respect to precipitation (i.e., annual precipitation-discharge hysteresis loops) is caused by transient water storage in the subsurface (Andermann et al., 2012). Precipitation reaching the surface is routed through storage compartments, which delays the drainage system response to precipitation. This delay results in a seasonal anticlockwise hysteresis with different river discharge at the end of the monsoon season than the pre-monsoon season even though both seasons are characterized by similar precipitation regimes. Thus, quantifying hysteresis may provide an alternative measure of transient water storage.

In this paper we apply multiple approaches to approximate storage variability in 242 medium to continental scale watersheds in monsoonal regions of Asia (hereafter “monsoon Asia”; Fig. 1), as defined by an independent definition of the monsoon (Wang and LinHo, 2002). We focus on monsoon Asia because of the relative simplicity of the hydrologic cycle; water input, and thus recharge, is restricted to the monsoon, which is effectively a long-lasting single annual event (Henck et al., 2010). We use daily and monthly precipitation and discharge data for watersheds (Fig. 1) to compare hysteresis terms to storage fluctuations derived from the Gravity Recovery And Climate Experiment (GRACE) satellite and river discharge recession curve analysis to understand what type of storage each of these measures represents. Because the different methods may quantify different storage processes, by comparing them we may obtain new insights into signals of storage in the hydrological cycle.

## 2. Background

### 2.1. Estimating storage

Over large scales ($>\sim 10^5$ km$^2$), gravity field measurements from the GRACE satellite allow direct observation of changes in terrestrial water storage and thus long wave seasonal cyclicity and temporal storage evolution (e.g., Strassberg et al., 2007). In these analyses, temporary, seasonal water storage is defined as the average amplitude of annual variations (Krakauer and Temimi, 2011) across the monsoon and non-monsoon seasons. We term this variation “transient storage”. GRACE measurements cannot distinguish between single storage units and thus integrate all water storage units (including ice, lakes, rivers, snow, biomass, soil moisture, and groundwater) over large areas, smoothing over small scale dynamics (Jiang et al., 2014). Furthermore, although extensive recent work has focused on using numeric hydrologic models to increase the spatial resolution of GRACE (Long et al., 2015), accurately and directly quantifying water storage at the watershed scale has remained elusive due to the difficulty in observing groundwater directly (Vorosmarty et al., 2013).

Another way to measure water storage in the landscape is by analyzing discharge recession curves to quantify groundwater contributions to river discharge (e.g., Brutsaert and Nieber, 1977). Long and undisturbed receding hydrographs after a period of water input (e.g. rainy monsoon season) are considered to be base flow periods that provide indirect information about the underlying storage volume (Brutsaert, 2008; Hall, 1968; Wittenberg, 1999). Evaluating recession curves allows researchers to estimate the dynamic variability of the groundwater head, or saturated zone, by assigning base flow discharge to the purging of the groundwater reservoir(s) (e.g., Brutsaert, 2005; Kirchner, 2009; Wittenberg, 1999). Dynamic storage quantifies water entering the system from groundwater with damped response times (Tallaksen, 1995), and thus is a measure of saturated zone water storage connected to the river network and its dynamic changes over time. We interpret the

clear seasonality and the very long characteristic end-of-season recession curve as a signal of seasonal loading and unloading of deep groundwater storage and term it "dynamic storage".

A prior study comparing GRACE-derived transient storage (GDTS) to recession curve derived dynamic storage in the continental United States finds that the two measures of storage are well-correlated but that regional estimates of GDTS exceed watershed estimates of recession curve derived dynamic storage by an order of magnitude (Krakauer and Temimi, 2011). They propose a number of explanations for the disparity, including scale issues between the local scale of recession analysis and regional scale of GRACE analysis, and conclude that no single factor dominates the disparity. An alternative interpretation could be that these metrics are not measuring the same storage compartments and thus, dynamic storage may be a part of transient storage rather than equivalent to it. Thus, to better understand how and why GDTS and recession curve derived dynamic storage are different, comparisons need to consider data from the same basins.

A third possible way to measure storage is through analysis of precipitation-discharge hysteresis loops ($P$-$Q$ hysteresis) (Andermann et al., 2012). Prior work in Nepal suggests that precipitation-discharge hysteresis is the result of the retardation of water entering rivers from precipitation due to intermediate groundwater storage in fractured bedrock (Andermann et al., 2012). Thus, systems with simple input-output relationships over the course of a year, such as monsoonal systems where most of the rainfall is concentrated in a well-defined wet season (e.g., Henck et al., 2010; Wang and LinHo, 2002), have P-Q hysteresis loops that may provide insight into the nature and dimensions of annual storage for the basin. The dimension (offset between the rising and falling limbs) of these hysteresis loops should scale with the storage capacity of the system and provide a quantification of annual storage variability.

### 2.2. Controls on water storage

Groundwater storage depends on the local bedrock geology, topography, and land cover of a watershed (e.g., Ilstedt et al., 2007; Krakauer and Temimi, 2011; Rodell et al., 2007; Sayama et al., 2011). A primary control on groundwater storage is the dynamic yield of the storage media, which depends on the porosity and volume of the storage compartment (Rodell et al., 2007) but is challenging to quantify. Storage may increase where slopes are steeper due to the increased space in fractures and porous rocks within the mountains (Sayama et al., 2011). Similarly, infiltration scales with basin steepness in some areas (Krakauer and Temimi, 2011) and steep terrain seems to route precipitation more efficiently into deep storage resulting in overall older water draining from these regions (Jasechko et al., 2016). In addition, we can infer from studies of the effects of deforestation, urbanization, and afforestation on infiltration and discharge that storage will increase for forested areas and decrease for urban areas (Ilstedt et al., 2007; Leopold, 1968). Furthermore, although the role of storage in ice and snow in high mountains receives widespread attention in central and western Asia (Pritchard, 2019) and play a major role in the local hydrologic cycle (Brun et al., 2017), at the continental scale snow and ice may play only a minor role as glaciers occupy only a small fraction of the large watersheds draining Asia.

## 3. Methods

### 3.1. Basin average precipitation, discharge, and evapotranspiration

Precipitation ($P$; [mm/day]) was extracted from the 0.25° APHRODITE dataset (Yatagai et al., 2012) because this is the most temporally and spatially accurate precipitation dataset for Asia and has the longest availability (e.g., Andermann et al., 2011). Although the entire study area is influenced by a summer monsoon, monsoon intensity and duration vary spatially and temporally. In order to define monsoon season parameters (onset, peak, withdrawal, duration) for each catchment directly from rainfall data, we applied the method of Wang and LinHo (2002). The method first aggregates the precipitation time series to an average annual five-day rain rate. These 73 pentads for each pixel are the basis for a Fourier regression. We then used the annual mean plus the first 12 Fourier harmonics to reconstruct a smoothed annual precipitation series. The monsoon characteristics for each precipitation pixel were determined using the intensity of the rainy season: the amplitude of annual variation and the ratio of summer to yearly rainfall. Average statistics for monsoon onset, peak, and withdrawal dates, as well as monsoon duration were then computed for each watershed. After calculating the monsoon duration for each pixel of the rainfall dataset, we limited analysis to watersheds with an average monsoon duration of at least one day. The reconstructed annual precipitation series of 73 pentads was used for stations with daily discharge data while aggregated monthly means were used for stations with monthly discharge data. The appropriate rainfall dataset (either monthly or 5-day smoothed) was then averaged for the upstream area of each station to calculate annual and monsoon precipitation for each watershed.

Discharge ($Q$; [mm/day]) data come from Chinese Hydrology Bureau (CHB, $n = 18$) (Henck et al., 2010), Mekong River Commission (MRC, $n = 57$) (MRC, 2015), and the Global Runoff Data Center (GRDC, $n = 167$) (GRDC, 2015) (Table S1). The GRDC data includes stations with daily ($n = 78$) and monthly ($n = 89$) data. Stations were located based on latitude and longitude data available from the data source. They were placed on the nearest river reach of the corresponding river delineated by HydroSHEDS (USGS, 2008). If the GIS-calculated upstream area was within 10% of the reported area of the station specifications then the station was used for analysis. GRDC data came with watersheds already delineated. To match the minimum resolution defined by the spatial resolution of the APHRODITE precipitation dataset (0.25°; ~30*30 km) we restricted our analysis to watersheds $\geq$1000 km$^2$ and with at least five years of data. Daily discharge ($Q$) data for each station was smoothed in the same way as the precipitation data (aggregation into an annual hydrograph of 73 pentads followed by a Fourier regression) resulting in 73 points of reconstructed data based on the annual mean plus the first 12 harmonics of the Fourier regression for each station. For stations with monthly data we calculated the mean discharge for each month over the entire period of record. For recession analysis we used the raw discharge data time series for stations with daily data and clear recession curves ($n = 105$).

In addition to precipitation and discharge, the final parameter to close the hydrological budget is evapotranspiration (ET; [mm/day]). ET is very difficult to measure *in situ* and depends on many parameters, including solar radiance, wind speed, bioactivity and temperature. Often ET is computed from more easily measurable parameters using semi-calibrated empirical models, e.g. Penman Monteith. Global meta-analyses report poor performance of global ET models (Liu et al., 2016; Trenberth et al., 2007); Liu et al. (2016) found that in humid areas, such as monsoon Asia, ET is significantly over estimated by available datasets. Trenberth et al. (2007) demonstrate that in ERA40, a global hydrological model, ET leads to impossible negative water balances and may even exceed precipitation. However, as ET is a fundamental component of the water cycle, we use the ET dataset identified by Liu et al. (2016) as the least inaccurate – Global Land Evaporation Amsterdam Model (GLEAM) (Martens et al., 2017). We processed the ET data the same way as the rainfall data and aggregated the data into 73 points for stations with daily data and monthly totals for stations with monthly data. The resulting water balance ($P - (Q + \mathrm{ET}) = \Delta S$

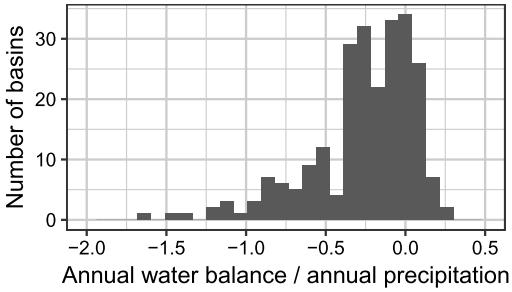


**Fig. 2.** Histogram showing the ratio of the annual water balance to annual precipitation. 2 basins with ratios $<-2$ are not shown. Annual water balance is normalized to precipitation to account for the huge range of annual precipitation values in the study basins. Water balances are largely negative in the study area.

where $S$ is storage), assuming net changes in storage are negligible, is negative for most watersheds (Fig. 2); 38 watersheds have annual water balances within 5% of the mean annual precipitation, 76 within 10%, and 114 within 20%. There is no statistically significant difference between the water balance for watersheds with daily or monthly data ($p = 0.75$, Mann Whitney U-Test).

### 3.2. Estimates of storage

To determine storage from GRACE satellite data, which we term "GRACE-derived transient storage" (GDTS hereafter, [mm/yr]), we used the JPL-Mascons RL05M GRACE product (Wiese et al., 2016), which is a 1° gridded dataset of variations in liquid water equivalent thickness from April 2002 to June 2017. We used JPL-Mascons monthly mass grids because it has previously been shown to be the most robust solution in comparison to physical measurements of changes in terrestrial water storage (Shamsudduha et al., 2017). We analyzed all five published GRACE solutions (three GRC Tellus solutions (Swenson, 2012), JPL-Mascons (Wiese et al., 2016), and GRGS (Luthcke et al., 2013)) and find that although there is some scatter, storage estimates are similar (Figs. S3-5). Analysis was limited to the 50 basins with areas $>10^5$ km$^2$. To determine mean annual transient storage from GRACE, we determined the average upstream GRACE value for each watershed for each data point for the entire time series. We calculated the amplitude of the GRACE signal in each year, or the transient water storage for the year, by subtracting the minimum GRACE value from the maximum (Fig. 3). We then averaged the amplitudes over all the analyzed years. Because there is only a single seasonal filling and emptying of the storage in this region of the world (due to the monsoon climate), we are able to use this annual storage metric as a measure of seasonal water storage.

We estimate dynamic storage following a long-established method that uses receding hydrographs to estimate groundwater storage in a catchment (Brutsaert and Nieber, 1977). We define dynamic storage as the water stored within the saturated zone of the catchment above zero flow level. This is the water stored above the lowest saturated groundwater head that is still hydrologically connected with the river network (e.g., Brutsaert, 2008). Dynamic storage ($S$; [mm/yr]) was calculated assuming a diffuse and slow purging aquifer producing discharge ($Q$; [mm/day]) normalized by the catchment area (e.g., Brutsaert, 2008; Kirchner, 2009), where $Q$ for dry periods depends on storage ($S$) and thus is a function of the negative change of $S$ over time,

$$Q = -\frac{dS}{dt} \tag{1}$$

We only consider time periods when precipitation ($P$; [mm/day]) $\approx 0$ and other losses of water (e.g. ET or groundwater seepage) from the system are negligible with respect to magnitude of $Q$ (Kirchner, 2009). Dynamic storage is also a function of $Q$ ($S = f(Q)$) during dry periods; as $Q$ drains the aquifer, $S$ decreases. We calculated $S$ for the 105 watersheds with daily data and a clearly definable recession periods (see below) by fitting a power law to the log-equal-spaced median bins in the $Q$ vs $\frac{dQ}{dt}$ space largely following the methods described by Kirchner (2009) for periods where discharge changes were negative. More details and theoretical considerations can be found in detailed work by Kirchner (2009) or the book by Brutsaert (2005):

$$-\frac{dQ}{dt} = aQ^b. \tag{2}$$

From this equation, Kirchner (2009) defines $dS$, which is the change in $S$ over a given time period (in this case the recession season), such that:

$$dS = \frac{dQ}{aQ^{b-1}}. \tag{3}$$

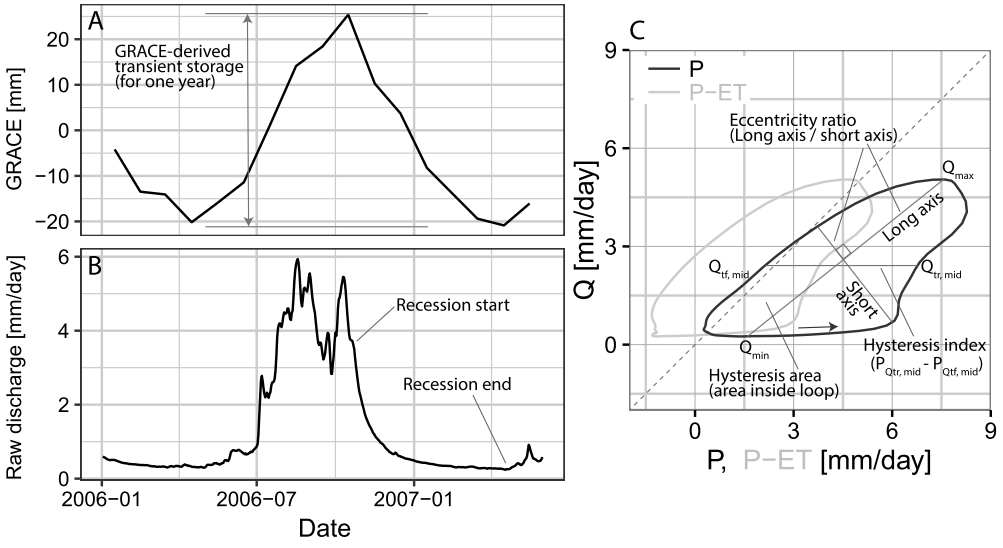


**Fig. 3.** Conceptual figure showing the definitions of storage terms used in this study. (A) GRACE storage for a single year. (B) A single recession curve used in the analysis. (C) Definition of hysteresis terms from smoothed precipitation and discharge data as well as the effects of ET on the hysteresis loop. Accounting for ET (the grey line) approximately corrects deviation from the 1:1 line. The arrow shows the direction of the precipitation-discharge hysteresis.

It is then possible to compute storage, $S$, by fitting equation (2) and numerically integrating equation (3) for $dS$. Thus, $dS$ can be derived from the change in river discharge ($dQ$) over a period of groundwater generated discharge.

In order to limit the influence of hydrologically relevant precipitation events and/or ET we selected recession periods through a rigorous process. 1) Recession periods needed to be outside the monsoon season of the catchment, as defined from precipitation data (see above). 2) Each recession segment needed to last at least five days. 3) The maximum accumulated rainfall during the post-monsoon recession must not exceed 60 mm. 4) Recession period discharge $Q$ must not exceed the maximum base flow index found using the generic digital base flow filtering method proposed by Eckhardt (2005). This last criterion provides an independent method of separating discharge into its flow components, with base flow assumed to be derived exclusively from slow groundwater storage. The annual change in storage, S, was calculated by numerically integrating equation 3 between the highest and lowest discharges of each recession period. We assume that the start and end of this long end-of-season recession spans the range of seasonal storage variations in the saturated zone; with one rainy season a year, this is the annual storage range as well. Reported dynamic storage values for each basin are the median of storage calculated for each annual recession period. See Fig. 3 for an example recession curve and the supporting information for more details about the analysis.

Filtering recession periods using the four conditions above gives us confidence that the recession period is minimally affected by ET. Treating ET properly in recession analysis is an ongoing issue and different authors have proposed different solutions, including using only nighttime data when sub-daily resolution data are available (e.g., Kirchner, 2009; Krakauer and Temimi, 2011). What we have done instead is to exclude data that is potentially influenced by ET through our strict definition of recession periods. In an ideal world we would estimate ET precisely and correct discharge, $Q$, for the missing volume in order to close the mass-balance of input (rain) as a function of output (discharge) for the entire system. However, this is not possible with the available ET data, as described above. While it is theoretically possible to explore the effect that not including ET has on the calculations, the poor performance of ET data for our region (only 42 of 105 watersheds used for dynamic storage calculations have annual water balances within 20% of the annual precipitation) and the commonly found negative water balance ($n = 88$ of the 105 watersheds used for dynamic storage calculations) preclude this analysis. In addition, we find that the most negative water balance numbers come from periods with the lowest rainfall, suggesting that the soil is dry on and near the surface and little to no water is available for continued evaporation. Because recession curve analysis measures the contribution of the saturated zone to discharge, analyses are made only for the dry season. Thus, ET is likely minimal and only related to evaporation off the river surface itself. Not considering ET and using daily data for recession curve analysis to determine storage (Brutsaert, 2008), recession time scales (Wittenberg, 1999), and estimate ET (assuming long-term constant storage) (Palmroth et al., 2010) is common in the literature, even for large watersheds (Peña-Arancibia et al., 2010).

Following Andermann et al. (2012) we propose precipitation-discharge hysteresis as a third approach to quantify storage. We define three terms to quantify the hysteresis effect by analyzing the shape and size of the P-Q hysteresis loop: the hysteresis area, hysteresis index (following Fovet et al., 2015), and eccentricity ratio (Fig. 3). For detailed explanation of the methods used to determine these terms, see the supporting materials (text and Fig. S1). To compare hysteresis-derived storage calculated using ET to storage estimated without including ET and determine if it is necessary to include ET in our calculations, we substituted $P\text{-}ET$ for $P$ in all calculations. In this case, we calculated the hysteresis area, hysteresis index, and eccentricity ratio from a plot of $Q$ as a function of $P\text{-}ET$. We then compared the hysteresis terms derived without including ET to those derived including ET using a linear regression. If ET has little effect on the data, the slope will be close to 1 and the $R^2$ value close to 1.

### 3.3. Basin average parameters

Basin-averaged parameters were determined using the watersheds delineated for each station. Upstream slope, area, and mean elevation were calculated from the 3″ HydroSHEDS DEM (USGS, 2008). Land use and land cover data come from the global gridded 10″ GlobCover dataset (Bontemps et al., 2013). Land cover and land use types were aggregated into shrubs/grassland, agricultural uses, forest, bare, and urban. We compared derived storage values to possible forcing parameters using linear regressions, with terms in log space when that improved the regressions. See table S1 for summary of watershed location, data source, and all topographic, climatic, and derived parameters for each watershed; Fig. S2 shows the distribution of these parameters across the study area.

## 4. Results

All derived storage parameters except eccentricity ratio have similar spatial distributions with the highest values in the lowlands of South and Southeast Asia and lowest on the topographic highland of the Tibetan Plateau, in China, and in northeast Asia (Fig. 4; Table S1); eccentricity ratio is inversely correlated with the other terms and thus shows the opposite trends. GDTS varies from 53.2 to 523.3 mm/yr ($n = 50$, mean = 312.1 mm/yr, standard deviation = 147.0 mm/yr) (Fig. 4A). GDTS increases from north to south across monsoon Asia, with the highest values in Southeast Asia. Excluding one outlier with dynamic storage >20,000 mm/yr, dynamic storage ranges from 2.48 to 3304.7 mm/yr ($n = 104$, mean = 118.8 mm/yr, standard deviation = 358.53 mm/yr) (Fig. 4B). Dynamic storage is highest in parts of Southeast Asia and on the Tibetan Plateau and lowest for Japan. Hysteresis area is highest in the Himalayas, parts of Southeast Asia, and the Philippines; lowest values are in eastern India, Tibet, central China, and Korea. Hysteresis index is less spatially varied; highest values are in eastern India and lowest in Tibet and Korea. Some hysteresis index values are apparently zero or negative for watersheds with short monsoons, small hysteresis, and only monthly data. Eccentricity ratio generally has the highest values in China, Tibet, and Pakistan with lower values to the northeast, in India, and in Southeast Asia.

Including ET in calculations of hysteresis terms has only a minimal effect on derived values, although most terms decrease slightly (Fig. 5). Hysteresis area is affected the least, and the most systematically, by including ET while eccentricity ratio is affected the most, and least systematically ($R^2 \geq 0.65$, $p < 0.01$, slope $\geq 0.71$).

GDTS and hysteresis terms are closely related to one another but independent of dynamic storage. Dynamic storage does not correlate with, and is an average of 7.3 ± 13.8 (0.01 to 76.6) times lower than, GDTS for the 31 stations with daily data which are also $\geq 10^5$ km$^2$ (and thus large enough to determine GDTS) (Fig. 6). Dynamic storage correlates only weakly with hysteresis area, hysteresis index, and eccentricity ratio ($R^2 \leq 0.10$); a multiple regression of dynamic storage as a function of these three terms only increases $R^2$ to 0.11 ($p < 0.01$). In contrast, GDTS correlates with hysteresis terms whether or not ET is included in calculations of hysteresis terms (Fig. 6). A multiple regression of GDTS as a function of the terms hysteresis index and eccentricity ratio explains

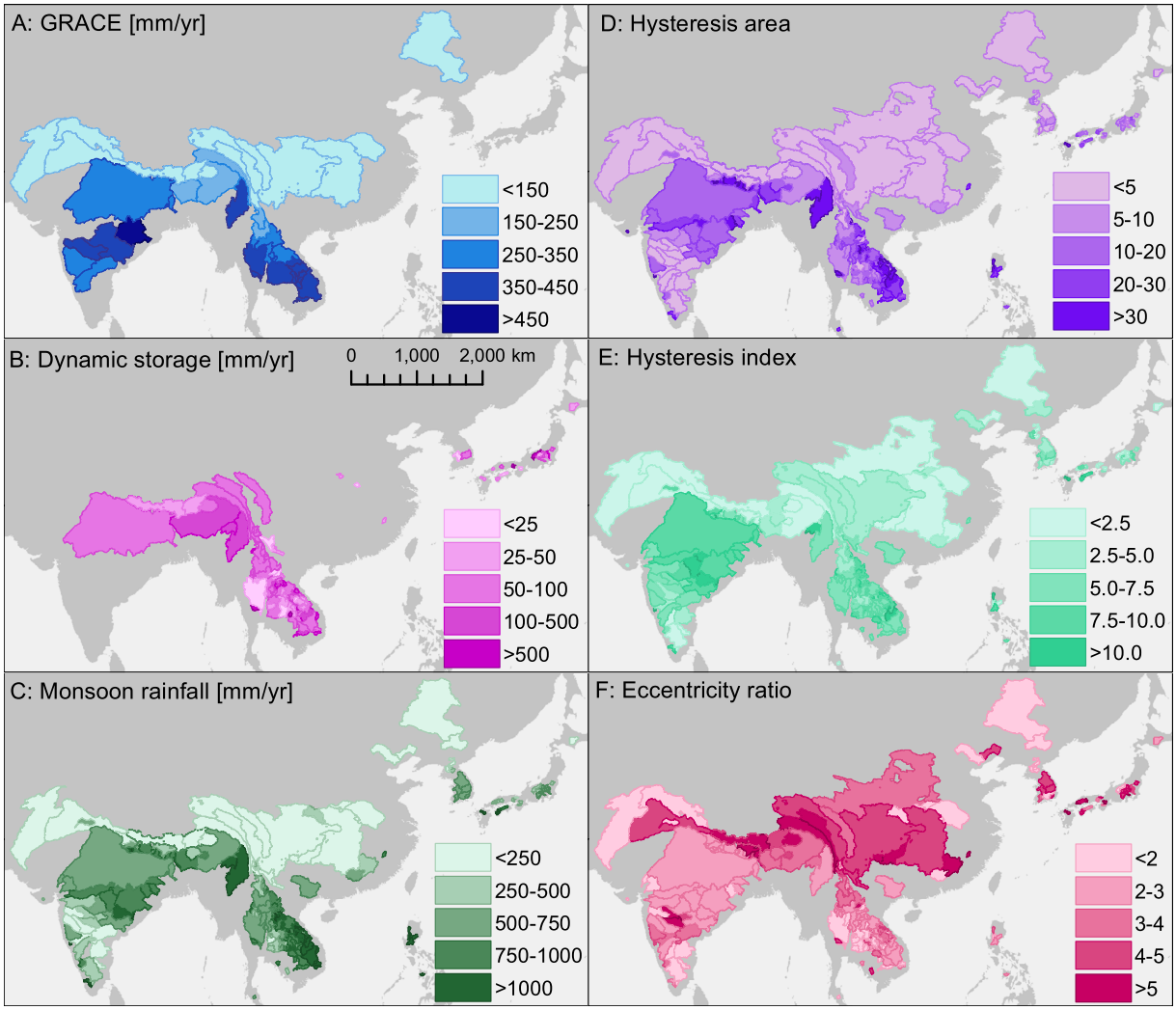


**Fig. 4.** Derived parameters for each watershed. Although the parameters derived represent the entire upstream area, many watersheds are nested, so only the unique area sampled by each station is shown. The data shown are: (A) GRACE-derived transient storage (GDTS), (B) dynamic storage, (C) monsoon rainfall, (D) hysteresis area, (E) hysteresis index, and (F) eccentricity ratio.

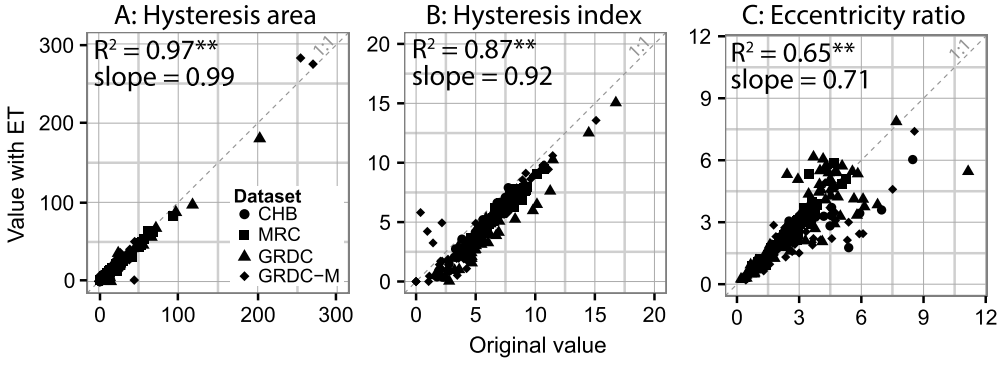


**Fig. 5.** Comparison of hysteresis terms derived without considering ET and when considering ET. The dashed line is the 1:1 line, where the original and the value with ET included are identical. ** for $p < 0.01$.

78% of the variance of the annual GRACE amplitude and is statistically significant for all terms and the intercept ($p < 0.05$):

$$\mathrm{GDTS} = 46.08\mathrm{HI} - 40.16\log(\mathrm{ER}) + 136.33 \quad (4)$$

where HI is the hysteresis index and ER is the eccentricity ratio. Including hysteresis area does not improve the correlation.

## 5. Discussion

We find that GDTS and hysteresis terms are independent, physically based measures of the same storage compartments but that dynamic storage represents only a subunit of this storage compartment. In this discussion, which we approach in a step-wise fashion, we first examine the effects of ET on hysteresis terms, then consider the possibility of estimating transient storage using hysteresis

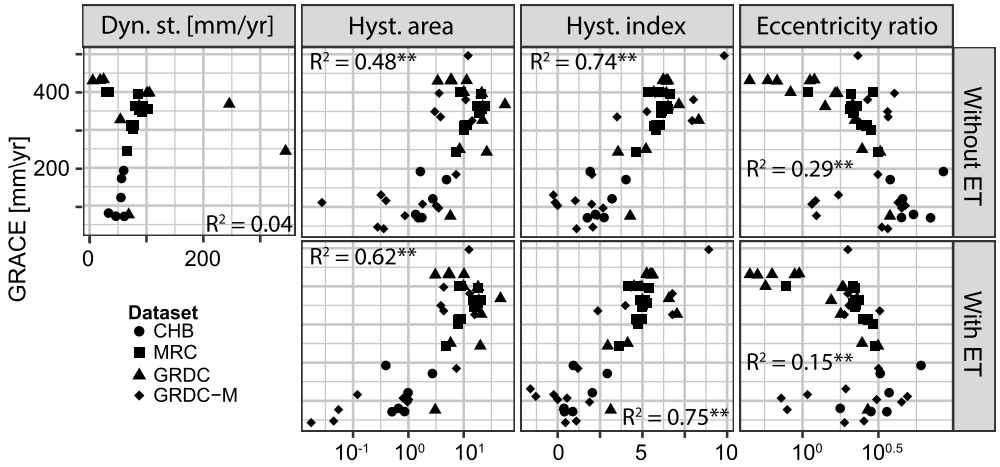


**Fig. 6.** Correlations among GRACE-derived transient storage (GDTS) and other derived parameters (both without [top row] and with [bottom row] ET considered) with $R^2$ for the regression on each panel; regressions are for what is shown (i.e., semi-log for hysteresis area and eccentricity ratio and linear for dynamic storage and hysteresis index). Dynamic storage was not calculated including ET data and is thus not shown. * for $p < 0.05$, ** for $p < 0.01$. All fits are included in Table S2.

terms scaled to GDTS, explore possible processes setting transient and dynamic storage, and then discuss the differences between transient storage and dynamic storage.

### 5.1. Effects of ET on hysteresis terms and correlations

Even though the water balance is heavily negatively skewed for the study region, all three hysteresis terms calculated with and without ET considered are strongly correlated to one another with slopes close to one (Fig. 5). These data suggest that the hysteresis terms are robust to not including ET in our calculations. The correlations between GDTS and all three hysteresis terms are similar whether ET is included or not for both single and multiple regressions (including two or three hysteresis terms; Table S2, Fig. 6). Overall our data suggest that even where ET is known to be overestimated for most watersheds, there is not a significant influence on the ability to use hysteresis terms to estimate storage and that not including ET is an appropriate simplification.

### 5.2. Estimating transient storage from hysteresis terms

We propose that transient storage can be estimated from eccentricity ratio and hysteresis index data scaled to GDTS using equation (4). Although a multiple regression that includes dynamic storage has a better correlation than those without, that would limit our analysis significantly both geographically and in number of watersheds because of the daily data needed for dynamic storage calculations. The large scale of the study area and thus the large variability of the environmental storage compartments (i.e., substrate variability) and the monthly data resolution for some stations likely explain much of the scatter in the correlation between hysteresis terms and GDTS. Evidence of this hypothesis is the better correlation for GDTS as a function of both hysteresis terms and dynamic storage that we get for watersheds with daily data available – the higher resolution of the data and the smaller geographic area of the watersheds with daily data improve the correlation.

Based on the good correlation between GDTS and hysteresis, we hypothesize that being able to estimate transient storage from precipitation-discharge hysteresis (hereafter hysteresis-derived transient storage, HDTS) may provide valuable a-priori information for downscaling GRACE satellite data for monsoon Asia to watersheds as small as the precipitation data resolution, $\sim 10^3$ km$^2$, and potentially even to smaller areas with higher resolution precipitation data. However, this method of estimating transient storage likely is only applicable for other regions with a well-defined rainy season or to the time span of single events. Because GRACE cannot be used reliably for areas $<10^5$ km$^2$, we are unable to directly test this hypothesis using the data in this study. Thus, future work should test the implicit assumption in our estimates that the processes controlling hysteresis and storage are the same across all scales, possibly by measuring transient storage directly, such as with GPS inversion (Fu et al., 2015) or gravimeter observations (Güntner et al., 2017). Previous work in Nepal, Western Australia, and California for watersheds ranging from $10^2$ to $10^5$ km$^2$ support the assumption that processes controlling hysteresis and storage are similar across watershed scales (Andermann et al., 2012; Müller et al., 2014).

In the study area, HDTS (derived using equation (4)) is lowest in mountainous areas draining the Tibetan Plateau and in central China and highest in northern India and SE Asia (Fig. 7). This broadly follows patterns of precipitation in the study region. Thus we argue that precipitation may be a first order control on patterns in transient storage. The low HDTS in mountainous areas may reflect the reduced capacity of the landscape to store surface water in shallow, transient storage. Shallow and undeveloped soils, sparse vegetation, and steep topography provide little storage capacity in the unsaturated zone and thus most water infiltrates into deep groundwater. This supports findings that high relief landscapes have overall older water, as determined from the isotopic signature (Jasechko et al., 2016) and emphasizes the importance of slow storage (e.g., ice and deep groundwater) in maintaining streamflow through the year in high relief regions.

### 5.3. Controls on water storage

Monsoon precipitation appears to be a strong direct control on HDTS but not dynamic storage. HDTS correlates well with monsoon precipitation ($R^2 = 0.39$, $p < 0.01$) while dynamic storage does not correlate strongly with any of the parameters we considered ($R^2 \leq 0.07$, $p > 0.05$) (Fig. 8). The good correlation of transient storage with monsoon precipitation is because they are autocorrelated: the rainfall input controls the amplitude change, thus increasing transient storage; pouring in more water will simply pile the water up higher in and on the landscape. In contrast, the poor correlation of dynamic storage and rainfall suggests that dynamic storage depends on other parameters, such as the storage media and infiltration rate into and from deep groundwater storage. Basin slope, a proxy for relief and thus potential storage space above the drainage base level set by rivers, does not correlate with either of our storage terms (Fig. 8), suggesting that storage is independent of basin topography on this large scale.

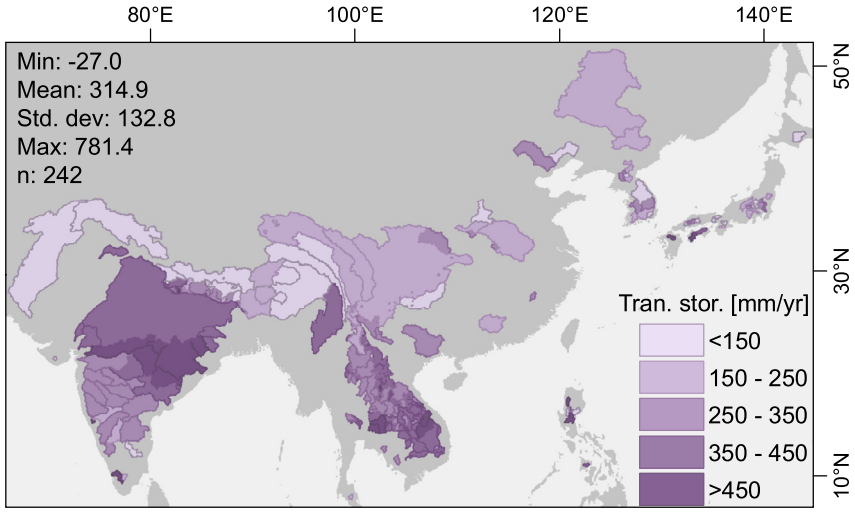


**Fig. 7.** Map of transient storage modeled using hysteresis index and eccentricity ratio scaled to GRACE (HDTS, hysteresis-derived transient storage in the text) using equation (4).

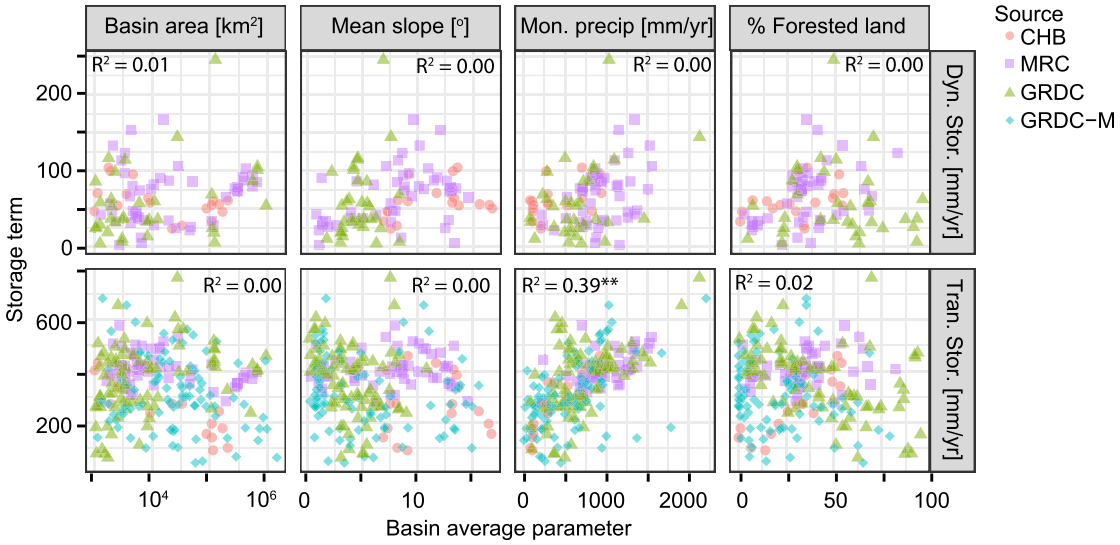


**Fig. 8.** Correlations between storage (dynamic storage (top) and hysteresis-derived transient storage (HDTS) (bottom)) and basin averaged parameters (from left to right: upstream area, average basin slope, monsoon rainfall, % forested land) with correlation statistics on each panel. Shape of the point identifies which dataset the basin is from. $R^2$ values are shown for each plot; * for $p < 0.05$, ** for $p < 0.01$. Two outliers with dynamic storage >300 mm/yr are not shown. For maps of the spatial distribution of these terms, see Fig. S2. Regression data are shown in Table S3.

Land use does not appear to play a significant role in setting either dynamic storage or HDTS (Fig. 8). However, we do see one location where land use may be altering the hydrologic cycle considerably. The eight watersheds with GRACE-derived storage >500 mm/yr are all clustered in two major watersheds draining northeastern and northwestern Thailand. These watersheds have uniformly low recession-derived dynamic storage and hysteresis area and are also outliers in the plots of GDTS against hysteresis index and eccentricity ratio. The region is heavily agricultural (primarily rice paddies) (86% in one watershed; 42% in the other) and has among the highest surface water irrigation rates (7% in one watershed, 13% in the other) in the entire study area (for entire area range is 0–25%; mean = 4.5%, standard deviation = 4.2%; irrigation data are from Siebert et al. (2013)). The watershed with more agriculture has lower rates of irrigation. Thus, we hypothesize that the surface irrigation in the region related to cultivating rice has artificially increased GDTS and may have altered other storage terms. In particular recharge rates of deep groundwater might be lower due to the massive exploitation of water for irrigation at the surface, potentially leading to enhanced evapotranspiration and consequently a net loss of water. Since the water is supplied to the landscape through rain but little actually contributes to groundwater and river discharge it will be detected by the integral GRACE signal but not by the other methods.

### 5.4. Differences between transient and dynamic storage

We propose that transient storage and dynamic storage are, although overlapping, measures of two different types of water storage and are not directly comparable. As with a prior study comparing GRACE and recession curve derived dynamic storage (Krakauer and Temimi, 2011), we find that transient storage is higher than dynamic storage (mean = 12.72, median = 7.26 times) (Fig. 9). Furthermore, transient storage and dynamic storage have different spatial patterns and different correlations with basin-average parameters. Given the relatively lower volume of dynamic storage compared to transient storage, we propose that dynamic storage primarily measures deeper groundwater fluxes producing baseflow. In contrast, transient storage appears to capture the in-

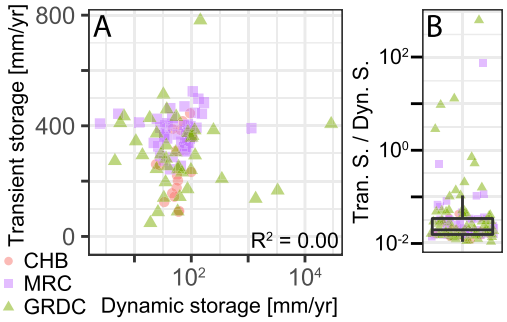


**Fig. 9.** Hysteresis-derived transient storage (HDTS) compared to dynamic storage. (A) Transient storage as a function of dynamic storage. (B) Ratio of HDTS to dynamic storage. Box boundaries are the 25th and 75th percentiles; the median is the centerline of the box. Whiskers extend to 1.5 times the range inside the box.

tegral changes of all water storage in the watershed, including dynamic storage, snow-pack, soil moisture, lakes, groundwater and loses due evapotranspiration. We infer that dynamic storage is only one component of transient storage and thus suggest that transient storage always, at a minimum, be equal to dynamic storage.

Our analysis suggests that transient and dynamic storage behave in fundamentally different ways. The correlation between monsoon precipitation and transient storage suggests that transient storage is input limited (i.e., more water added means there is more storage). In contrast, the poor correlation between dynamic storage and monsoon precipitation suggests that dynamic storage does not directly depend on rainfall patterns but depends instead on the connectivity between the surface and deep subsurface. With respect to size and volume, the deep saturated groundwater zone has a much larger capacity than the vadose zone and is presumably at least several times greater than the annual input volume, and dynamic storage is only the smaller seasonal amplitude of change. We interpret deep groundwater as a simple leaky bucket system that is always dynamically connected to river channels. Groundwater discharge into rivers depends directly on the height of the hydrological head and the transmissivity of the system. Deep groundwater is loaded by recharge and thus discharge into river channels increases. This implies that a large range of storage variability is relatively difficult to obtain without the vadose zone and land surface being dynamically connected to the channel network. Together with water losses due to ET the leaky bucket can explain why transient storage is an average of seven times greater than dynamic storage. Furthermore, our data suggest that continental scale storage variability in this wet environment is dominated by storage close to the surface rather than by the saturated zone. This finding is supported by recent work in the United States that found that subsurface water storage includes direct storage that contributes to streamflow (our dynamic storage) as well as indirect storage which cannot be resolved from streamflow (and is included in our transient storage) (Dralle et al., 2018).

Although dynamic storage is only a fraction of the volume of transient storage, it plays a fundamental role in controlling annual streamflow. Without deep dynamic storage contributing water to discharge through dry seasons, water would not be available in rivers for the variety of ecosystem services it provides, including habitat and human use. The rate of water transfer from the surface through soils and the vadose zone is fundamentally important to maintaining discharge in rivers (e.g., Dralle et al., 2018; Rempe and Dietrich, 2018). Our results demonstrate that storage of water on the landscape scale can be grouped into two compartments: 1) the highly dynamic transient storage acting as a transfer filter for 2) the deep saturated dynamic storage driving river discharge through the dry season. Thus, because volume of water input by precipitation is not directly reflected in dynamic storage, dynamic storage

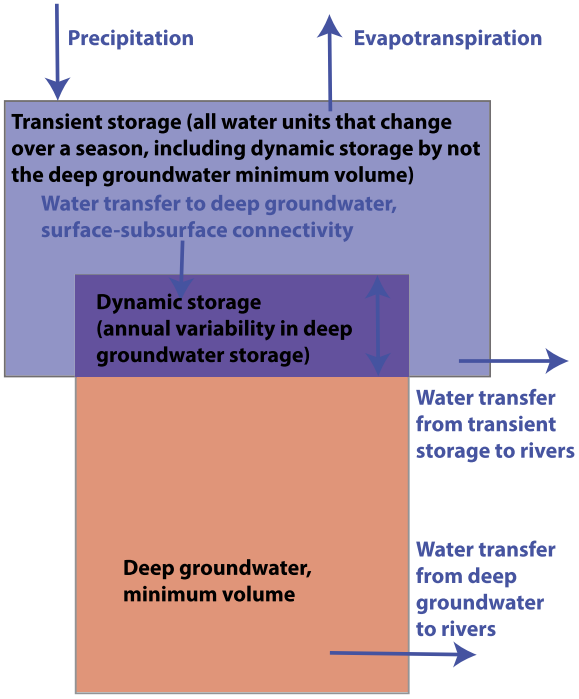


**Fig. 10.** Conceptual model of how transient storage, dynamic storage, and deep groundwater storage are related. Theoretically dynamic storage could go all the way to the surface.

seems to be an intermediate buffer for terrestrial water storage and, thus, resources. Ultimately, surface and shallow subsurface properties control the rates of seasonal recharge and response of the river system to precipitation input. Understanding the dynamics of transient storage is crucial for water resource management in order to ensure continuity of water availability throughout the year.

## 6. Conclusions

We estimated storage using GRACE, recession curve analysis, and precipitation-discharge hysteresis for 242 watersheds ranging in size from $10^3$ to $10^6$ km$^2$ in Asia. Hysteresis terms correlate well with GRACE-derived transient storage. We propose that this correlation may be able to be used to estimate transient storage for watersheds as small as $10^3$ km$^2$ (the scale of our precipitation data) from precipitation and discharge observations without relying on models. These independent observations of storage variation and, thus, temporal distribution of mass could be used by both GRACE product developers and users as a-priori information to downscale GRACE in regions with strongly seasonal rainfall.

Using the observed relationship between GRACE and hysteresis terms, we argue that the different storage compartments likely undergo independent dynamic behavior. We find that transient storage derived from hysteresis terms is a factor of seven higher than, and correlates poorly with, hydrograph recession curve derived dynamic storage. This implies that fluctuations within the saturated zone are considerably smaller than transient water storage in the vadose zone and on the surface. We propose that dynamic storage is lower than transient storage because it is part, but not all, of the water measured by transient storage (Fig. 10). Transient storage includes changes in lake levels, soil moisture, snow pack, shallow groundwater, and biomass, while dynamic storage likely only measures the annual variability in deep groundwater contributing to streamflow. Furthermore, we find that transient storage only correlates with monsoon rainfall, suggesting that transient storage is input limited. In contrast, dynamic storage does not correlate with

any considered parameters, suggesting that dynamic storage is not directly connected to the surface and the fluctuations are mediated by processes within the vadose zone. Thus, water input by precipitation is an important control on transient storage variability, suggesting that transient storage is sensitive to both interannual and longer time scale variations in precipitation. Our findings support the concept of a leaky bucket across several orders of magnitude in locations where discharge during dry seasons depends directly on the groundwater level.

## Declaration of competing interest

The authors declare that they have no known competing financial interests or personal relationships that could have appeared to influence the work reported in this paper.

## Acknowledgements

The authors thank A. Gilliom for early work on this project. Discussions with J. Turowski and L. Longuevergne were helpful in clarifying ideas presented here. Thanks for P. Bierman, K. Danner, K. Cook, and three anonymous reviewers for comments on early drafts. C. Andermann benefitted from the Helmholtz Postdoc Program (PD-039) from the German Helmholtz Association. GRACE land data are available at http://grace.jpl.nasa.gov, supported by the NASA MEaSUREs Program. Discharge data are available directly from the sources cited in the paper – we are not authorized to share these data.

## Appendix A. Supplementary material

Supplementary material related to this article can be found online at https://doi.org/10.1016/j.epsl.2020.116415.

## References

Andermann, C., Bonnet, S., Gloaguen, R., 2011. Evaluation of precipitation data sets along the Himalayan front. Geochem. Geophys. Geosyst. 12 (7).
Andermann, C., Longuevergne, L., Bonnet, S., Crave, A., Davy, P., Gloaguen, R., 2012. Impact of transient groundwater storage on the discharge of Himalayan rivers. Nat. Geosci. 5 (2), 127–132.
Bontemps, S., Defourny, P., Radoux, J., Van Bogaert, E., Lamarche, C., Archard, F., Mayaux, P., Boettcher, M., Brockmann, C., Kirches, G., Zulkhe, M., Kalogirou, V., Arino, O., 2013. Consistent global land cover maps for climate modeling communities: current achievements of the ESA's land cover CCI. In: Proceedings ESA Living Planet Symposium. Edinburgh, United Kingdom, 9–13 September.
Brun, F., Berthier, E., Wagnon, P., Kääb, A., Treichler, D., 2017. A spatially resolved estimate of High Mountain Asia glacier mass balances from 2000 to 2016. Nat. Geosci. 10 (9), 668–673.
Brutsaert, W., 2005. Hydrology: An Introduction. Cambridge University Press.
Brutsaert, W., 2008. Long-term groundwater storage trends estimated from streamflow records: climatic perspective. Water Resour. Res. 44 (2).
Brutsaert, W., Nieber, J.L., 1977. Regionalized drought flow hydrographs from a mature glaciated plateau. Water Resour. Res. 13 (3), 637–643.
Dralle, D.N., Hahm, W.J., Rempe, D.M., Karst, N.J., Thompson, S.E., Dietrich, W.E., 2018. Quantification of the seasonal hillslope water storage that does not drive streamflow. Hydrol. Process. 32 (13), 1978–1992.
Eckhardt, K., 2005. How to construct recursive digital filters for baseflow separation. Hydrol. Process. 19 (2), 507–515.
Fovet, O., Ruiz, L., Hrachowitz, M., Faucheux, M., Gascuel-Odoux, C., 2015. Hydrological hysteresis and its value for assessing process consistency in catchment conceptual models. Hydrol. Earth Syst. Sci. 19 (1), 105–123.
Fu, Y., Argus, D.F., Landerer, F.W., 2015. GPS as an independent measurement to estimate terrestrial water storage variations in Washington and Oregon. J. Geophys. Res., Solid Earth 120 (1), 552–566.
Gleeson, T., Befus, K.M., Jasechko, S., Luijendijk, E., Bayani Cardenas, M., 2016. The global volume and distribution of modern groundwater. Nat. Geosci. 9, 161–167.
GRDC, 2015. Mean monthly discharges. In: Centre, G.R.D. (Ed.), Koblenz. Federal Institute of Hydrology (BfG).
Güntner, A., Reich, M., Mikolaj, M., Creutzfeldt, B., Schroeder, S., Wziontek, H., 2017. Landscape-scale water balance monitoring with an iGrav superconducting gravimeter in a field enclosure. In: Proceedings EGU General Assembly Conference Abstracts, vol. 19, p. 13940.
Hall, F.R., 1968. Base-flow recessions-a review. Water Resour. Res. 4 (5), 973.
Henck, A., Montgomery, D.R., Huntington, K.W., Liang, C., 2010. Monsoon control of effective discharge, Yunnan and Tibet. Geology 38 (11), 975–978.
Ilstedt, U., Malmer, A., Verbeeten, E., Murdiyarso, D., 2007. The effect of afforestation on water infiltration in the tropics: a systematic review and meta-analysis. For. Ecol. Manag. 251 (1), 45–51.
Jasechko, S., Kirchner, J.W., Welker, J.M., McDonnell, J.J., 2016. Substantial proportion of global streamflow less than three months old. Nat. Geosci. 9, 126–129.
Jiang, D., Wang, J., Huang, Y., Zhou, K., Ding, X., Fu, J., 2014. The review of GRACE data applications in terrestrial hydrology monitoring. Adv. Meteorol.
Kirchner, J.W., 2009. Catchments as simple dynamical systems: catchment characterization, rainfall-runoff modeling, and doing hydrology backward. Water Resour. Res. 45.
Krakauer, N.Y., Temimi, M., 2011. Stream recession curves and storage variability in small watersheds. Hydrol. Earth Syst. Sci. 15 (7), 2377–2389.
Leopold, L.B., 1968. Hydrology for Urban Land Planning: A Guidebook on the Hydrologic Effects of Urban Land Use.
Liu, W., Wang, L., Zhou, J., Li, Y., Sun, F., Fu, G., Li, X., Sang, Y.-F., 2016. A worldwide evaluation of basin-scale evapotranspiration estimates against the water balance method. J. Hydrol. 538, 82–95.
Long, D., Longuevergne, L., Scanlon, B.R., 2015. Global analysis of approaches for deriving total water storage changes from GRACE satellites. Water Resour. Res. 51 (4), 2574–2594.
Luthcke, S.B., Sabaka, T., Loomis, B., Arendt, A., McCarthy, J., Camp, J., 2013. Antarctica, Greenland and Gulf of Alaska land-ice evolution from an iterated GRACE global mascon solution. J. Glaciol. 59 (216), 613–631.
Manabe, S., 1969. Climate and the ocean circulation, I: the atmospheric circulation and the hydrology of the earth's surface. Mon. Weather Rev. 97 (11), 739–774.
Martens, B., Miralles, D.G., Lievens, H., van der Schalie, R., de Jeu, R.A.M., Fernández-Prieto, D., Beck, H.E., Dorigo, W.A., Verhoest, N.E.C., 2017. GLEAM v3: satellite-based land evaporation and root-zone soil moisture. Geosci. Model Dev. 10 (5), 1903–1925.
McDonnell, J.J., 2017. Beyond the water balance. Nat. Geosci. 10 (6), 396.
MRC, 2015. Hydrology and river monitoring. In: Commissions, M.R. (Ed.), Vientiane, Mekong River Commission.
Müller, M.F., Dralle, D.N., Thompson, S.E., 2014. Analytical model for flow duration curves in seasonally dry climates. Water Resour. Res. 50 (7), 5510–5531.
Oki, T., Kanae, S., 2006. Global hydrological cycles and world water resources. Science 313 (5790), 1068–1072.
Palmroth, S., Katul, G.G., Hui, D., McCarthy, H.R., Jackson, R.B., Oren, R., 2010. Estimation of long-term basin scale evapotranspiration from streamflow time series. Water Resour. Res. 46 (10).
Peña-Arancibia, J., Van Dijk, A., Mulligan, M., Bruijnzeel, L.A., 2010. The role of climatic and terrain attributes in estimating baseflow recession in tropical catchments. Hydrol. Earth Syst. Sci. 14 (11), 2193–2205.
Pritchard, H.D., 2019. Asia's shrinking glaciers protect large populations from drought stress. Nature 569 (7758), 649–654.
Rempe, D.M., Dietrich, W.E., 2018. Direct observations of rock moisture, a hidden component of the hydrologic cycle. Proc. Natl. Acad. Sci. USA 115 (11), 2664–2669.
Rodell, M., Chen, J.L., Kato, H., Famiglietti, J.S., Nigro, J., Wilson, C.R., 2007. Estimating groundwater storage changes in the Mississippi River basin (USA) using GRACE. Hydrogeol. J. 15 (1), 159–166.
Sayama, T., McDonnell, J.J., Dhakal, A., Sullivan, K., 2011. How much water can a watershed store?. Hydrol. Process. 25 (25), 3899–3908.
Scanlon, B.R., Zhang, Z., Save, H., Sun, A.Y., Müller Schmied, H., van Beek, L.P.H., Wiese, D.N., Wada, Y., Long, D., Reedy, R.C., Longuevergne, L., Döll, P., Bierkens, M.F.P., 2018. Global models underestimate large decadal declining and rising water storage trends relative to GRACE satellite data. Proc. Natl. Acad. Sci. USA.
Shamsudduha, M., Taylor, R.G., Jones, D., Longuevergne, L., Owor, M., Tindimugaya, C., 2017. Recent changes in terrestrial water storage in the Upper Nile Basin: an evaluation of commonly used gridded GRACE products. Hydrol. Earth Syst. Sci. 21 (9), 4533–4549.
Siebert, S., Henrich, V., Frenken, K., Burke, J., 2013. Global map of irrigation areas, version 5. In: Nations, RF-W-UFaAOotU. Bonn, Germany/Rome, Italy.
Strassberg, G., Scanlon, B.R., Rodell, M., 2007. Comparison of seasonal terrestrial water storage variations from GRACE with groundwater-level measurements from the High Plains Aquifer (USA). Geophys. Res. Lett. 34 (14).
Swenson, S., 2012. GRACE Monthly Land Water Mass Grids NETCDF, Release 5.0, Ver. 5.0. PO. DAAC, CA, USA, Vol. 2018.
Tallaksen, L., 1995. A review of baseflow recession analysis. J. Hydrol. 165 (1–4), 349–370.
Taylor, R.G., Scanlon, B., Doll, P., Rodell, M., van Beek, R., Wada, Y., Longuevergne, L., Leblanc, M., Famiglietti, J.S., Edmunds, M., Konikow, L., Green, T.R., Chen, J.Y., Taniguchi, M., Bierkens, M.F.P., MacDonald, A., Fan, Y., Maxwell, R.M., Yechieli, Y., Gurdak, J.J., Allen, D.M., Shamsudduha, M., Hiscock, K., Yeh, P.J.F., Holman, I., Treidel, H., 2013. Ground water and climate change. Nat. Clim. Change 3, 322–329.
Trenberth, K.E., Smith, L., Qian, T., Dai, A., Fasullo, J., 2007. Estimates of the global water budget and its annual cycle using observational and model data. J. Hydrometeorol. 8 (4), 758–769.

USGS, 2008. HydroSHEDS: World Wildlife Fund (WWF). v. online: http://hydrosheds.cr.usgs.gov/. (Accessed 22 January 2009).
Vorosmarty, C.J., Pahl-Wostl, C., Bhaduri, A., 2013. Water in the anthropocene: new perspectives for global sustainability. Curr. Opin. Environ. Sustain. 5 (6), 535–538.
Wang, B., LinHo, 2002. Rainy season of the Asian-Pacific summer monsoon. J. Climate 15 (4), 386–398.
Wiese, D.N., Landerer, F.W., Watkins, M.M., 2016. Quantifying and reducing leakage errors in the JPL RL05M GRACE mascon solution. Water Resour. Res. 52 (9), 7490–7502.
Wittenberg, H., 1999. Baseflow recession and recharge as nonlinear storage processes. Hydrol. Process. 13 (5), 715–726.
Yatagai, A., Kamiguchi, K., Arakawa, O., Hamada, A., Yasutomi, N., Kitoh, A., 2012. APHRODITE: constructing a long-term daily gridded precipitation dataset for Asia based on a dense network of rain gauges. Bull. Am. Meteorol. Soc. 93 (9), 1401–1415.